Journal of Theoretical and Applied Information Technology
15th March 2017. Vol.95. No 5

ISSN: 1992-8645 www.jatit.org E-ISSN: 1817-3195

BAG-OF-SHAPES DESCRIPTOR USING SHAPE ASSOCIATION BASED ON FREEMAN CHAIN CODE

[1]EMA RACHMAWATI, [2]IPING SUPRIANA, [3]MASAYU L. KHODRA

[1,2,3]School of Electrical Engineering and Informatics, Institut Teknologi Bandung, Indonesia

[1]ema.rachmawati22@students.itb.ac.id, [2]iping@stei.itb.ac.id, [3]masayu@stei.itb.ac.id

ABSTRACT

A novel bag-of-shapes descriptor constructed using shape association is presented in this paper. We believe that shape association has significant impact in constructing better shape representation of object, for the purpose of object recognition. In our proposed model, shape association is represented in the set of representative prototypes, which is generated through K-medoids clustering based on association likelihoods. The association likelihood is obtained through pairwise distance computation using Needleman-Wunsch algorithm, as the shape is represented in sequence of code of Freeman Chain Code. We evaluate our method on a set of 32 fruit subcategories captured in multi viewpoint. We show that our approach can reliably classify the shape of multi-class fruit with average accuracy of 82.96 % using nearest neighbor classifier.

Keywords: *Bag-of-Shapes, Freeman Chain Code, Shape Association, K-medoids clustering, Needleman-Wunsch Algorithm, Nearest Neighbor Classifier*

1. INTRODUCTION

Representing the shape of object in digital images has been recognized as a difficult task, whereas shape is undoubtedly as an important visual feature. According to this, there were many shape representation approaches developed so far [1][2][3][4]. Meanwhile, it is widely known that to represent an object contour we can use the chain code representation. Chain code as a structural based shape representation, has advantages in handling occlusion problem and allowing partial matching [1]. Chain code is an approach that is widely used to represent digital curves in image analysis, by describing the movement along a digital curve using 8-connectivity or 4-connectivity neighborhood. There were many application which use chain code representation to represent the boundary of geometric shapes, namely [5]–[7] to name a few. Azmi and Nasien [5] used chain code to extract feature of English character. Park et al. [6] also used chain code to represent contour of the object in their application as well. Also, the chain code was used in [7] for a real application in a car plates recognition system.

On the other hand, the concept of representing categories using ideal examples or prototypes rather than a set of formal logical rules, has been stated long time ago[8]. For example, a Mercedes is more likely prototype for the category of car; a less likely choice might be a bicycle. Furthermore, the use of object associations based on evidence of cognitive science, in which generally the problem of recognition is not centered on 'What is that?', but more likely 'Similar to what?' [9].

In this article, we adopt the successful idea of object association on the classical shape representation, in the form of chain code representation. We proposed a novel bag-of-shapes descriptor using shape association which is constructed based on Freeman Chain Code [10]. We apply k-medoids clustering [11] to get some prototypes/exemplars of each object class. Beforehand, from the chain code representation of object contour, we calculate a likelihood association using Needleman-Wunsch algorithm. From the experiment on the multiclass fruit dataset, we successfully show that the proposed descriptor has significant effect in improving the recognition result.

The remainder of the article is organized as follows. In Section 2, we briefly explained some works related to our work. Detail explanation of our proposed model can be seen in Section 3. The dataset and experimental evaluation can be seen in Section 4 while conclusion described in Section 5.

2. RELATED WORKS

Usually, object recognition is assumed to mean 'object naming' – given an image, the goal is to give the proper name to the objects in the image [12]. Giving a name to every possible object instance in the image is seemed to be difficult, this requires object categories used in the naming process. On the other hand, using object association in object recognition is more beneficial than using object naming, in which there is no need to segment the object into a pre-defined category. Instead, to infer the identity of each instance of the object, we only need to use its nearest neighbor (nearest neighbor) instance. Lately, some of the system shows that the simple approach using KNN can demonstrate excellent performance [13].

Belongie et al. [14] and Zhang and Malik [15] has applied the object association in their research. Belongie et al. [14] created shape context descriptor and implement it in object recognition problem. They applied chi-square [16] to calculate the distance between two closest points in two different shapes. Further, the k-medoids clustering is used to select some prototypes/exemplars from each class, as the representation of each class. The shape context descriptor also used by Zhang and Malik [15] as the shape representation in the object recognition problem. For the purpose of getting some shape representation, they also applied K-medoids for choosing prototypes in each object class. In order to get an approximation of the distance of two shapes, they just sum over the shape context distance.

On the other hand, for the purpose of object recognition based on chain code representation, Iivarinen and Visa construct a chain code histogram (CCH) [17]. CCH is the simplest technique used in matching chain code representation. The CCH is defined as $h_i = n_i/N$, where n_i is the number of chain code with i-direction, and N is the number of links. The CCH reflects the probabilities of different directions present in a contour. Though it is said that CCH is translation and scale invariant, but it is only invariant to a rotation of 90° [1]. Also, it did not consider the direction distribution in a chain code sequence [18]. Furthermore, the CCH also suffer from the noise sensitivity problem [1]. Some approaches has been taken to overcome the limitation of CCH, namely CCDV [19], CCRE [20] to name a few. In general, those three approaches successfully able to improve the weakness of CCH by conducting some modification in the construction of chain code.

In contrast with the way used in CCH [17] in utilizing the chain code representation for the shape contour, CCDV [19] and CCRE [20] improve the power of CCH by adding particular functionality based on statistical, distribution, and spatial property of chain code. The order difference of each chain code is used as the distribution feature in CCDV [19]. They define the order variance by proposing a new distance definition in chain code sequence. The order of each direction code in its sequence is defined as its distance to the first code, hence the first chain code distance is zero. Further, in the chain code histogram of a particular shape contour, they add this particular order variance. Meanwhile, the authors in CCRE [20] introduce a relativity histogram in addition to the chain code histogram. They adopted the transition probability of Markov chain in the construction of relativity histogram. Though these methods proved to achieve higher performance compared to CCH, however, these methods still suffered from the limitation of chain code. The same object, might reflect many different shapes depend on the camera viewpoint in the acquiring process. This condition might generate different chain code sequences, hence, might be recognized as different object.

Although in this article we also exploit the chain code representation to represent the shape contour, our work is different from the work in [17], [19], [20]. The authors in [17] only consider the probabilities of different directions present in a contour. In [19], [20], the authors improved the weakness of applying the chain code by adding some modification in the construction of chain code histogram. In contrast with their work, we do not construct nor modify the chain code histogram. Instead, we extract the shape association of shape contour using their chain code representation.

In this article, we adopt the idea of Shuo et al. [21] in using bag-of-shapes for shape descriptor in object recognition. Shuo et al. [21] proposed bag-of-shape descriptor for medical imaging. They used likelihood association based on blog, homogeneity, and edge, as they represent the shape as closed region. It is differed from the work of [21] though we adopt the term bag-of-shapes from their article. Since our work focuses on shape contour, hence, we conduct some preprocessing steps in order to get the shape contour. Furthermore, our work use likelihood association based on Needleman-Wunsch sequence alignment algorithm. Further, to get the shape correspondence/association we apply the k-medoids clustering to the result of likelihood association.

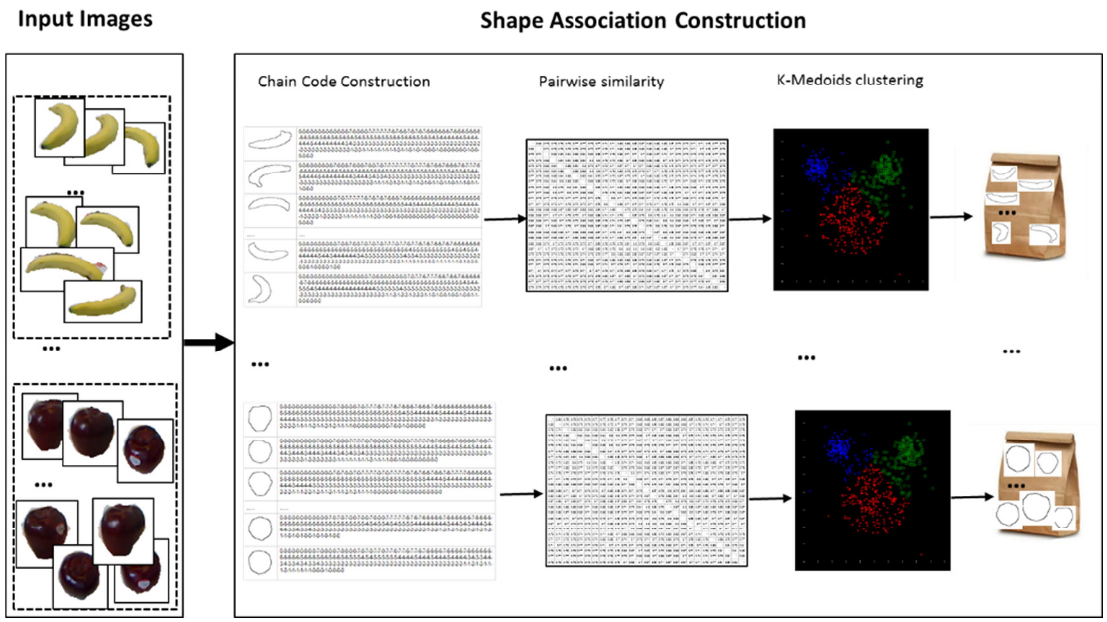

Figure 1: Illustration of bag-of-shapes descriptor construction

3. BAG-OF-SHAPES USING SHAPE ASSOCIATION

In this section we describe the construction of shape descriptor, which is bag-of-shapes descriptor using shape association. The abstraction of our proposed descriptor can be seen in Figure 1. In general, the process of constructing the bag-of-shapes is as follows:

(a) Chain code construction,
(b) Shape association construction in each fruit subcategory,
(c) K-medoids clustering on the result of (b), and extraction of k-cluster medoids and use them as the bag-of-shapes descriptor.

A more detail explanation is given in Section 3.1, 3.2, and 3.3.

3.1 Chain Code Construction

As we only need the contour of fruit object, we only use the cropped images version of the dataset, which contain the foreground object only [22]. Canny edge detection [23] was applied to those cropped color images to detect boundary of fruit object. This process yielded edge binary map.

Further, we conduct thinning process on edge binary map using a thinning algorithm [24]. Then we traced the contour [25] of one-thick pixel to construct shape representation in the form of chain code. An 8-connectivity Freeman Chain Code [10] is used to represent the contour of object because of its simple and compact form of data representation and its suitability for fast processing. Further we use the chain code for representing the shape of fruit object. The process of chain code construction explained above is depicted in Figure 2.

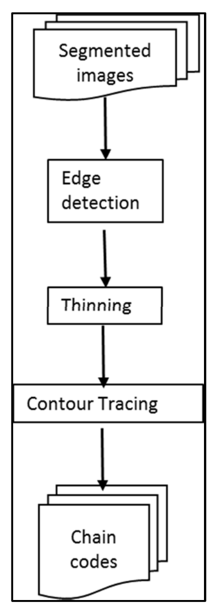

Figure 2: Illustration Of Chain Code Construction

3.2 Shape Association Construction

After we get the chain code of each fruit object contour, we compute the pairwise shape similarity using chain code string as shape representation. This process is conducted for each fruit subcategories.

Here, we give the definition of bag-of-shapes descriptor using shape association. A shape descriptor of an image I, $S(I)$, can be defined as a vector with k-dimension, according to bag-of-shapes as depicted in (1),

$$S(I) = \{A_I^1, A_I^2, A_I^3, \dots, A_I^n\} \quad (1)$$

where A_I^n is the shape association likelihood between shape in I and the nth shape, S_n. The shape association between an image I and a certain shape S, is measured using Needleman-Wunsch algorithm.

Basically, in Freeman Chain Code, each object contour was represented as a sequence over a finite alphabet [10]. Hence, the Needleman-Wunsch global alignment algorithm [26] was used to estimate the similarity between two sequences. Readers can refer to our article in [27] to further study the implementation example of this algorithm.

In applying Needleman-Wunsch algorithm to our model, we conduct a modification in the substitution cost (or scoring function) over each pair of possible sequence alphabet, e.g., the cost of substituting alphabet '0' with alphabet '1'. Because each alphabet in the chain code sequence having particular meaning, hence, in this paper, we did not use the common scoring function already defined in Bioinformatics domain [28], [29]. Instead, we define our scoring function, according to the characteristics of each alphabet of the chain code itself. As each code contains its particular direction, hence, we adopt the scoring function (σ) of [27] as can be seen in (2),

$$\begin{aligned} &if\ C_1(i) = C_2(j)\ then \\ &\qquad \sigma\big(C_1(i), C_2(j)\big) = \mathrm{w}(i,j) \times 1 \\ &else \\ &\qquad \sigma\big(C_1(i), C_2(j)\big) = \mathrm{w}(i,j) \times -1 \end{aligned} \quad (2)$$

where $C_n(i)$ is ith alphabet of string of chain code n, $w(i,j)$ is the cost for matching each pair of alphabet as can be seen in (3), where $\{i,j \mid 0,..7\}$.

$$\mathrm{w}(i,j) = \begin{cases} 1 & ,i = j \\ \dfrac{|i-j|}{4} & ,|i-j| \leq 4 \\ 1 - \dfrac{|i-j|-4}{4} & ,|i-j| > 4 \end{cases} \quad (3)$$

We normalize the shape association score in the range 0 – 1. If the score close to 1, it means the two sequences is similar, and vice versa.

3.3 K-Medoids Clustering in the Bag-of-Shapes Descriptor Construction

Technically, the shape association construction in Section 3.2 will produce a matrix containing pairwise-similarity value for each fruit category. In order to get the fruit prototypes, further, we apply K-medoids clustering [11] to select k-representative prototypes for each fruit category. K-medoids minimizes the sum of dissimilarities between points as member of a cluster and the center of that cluster. In contrast to the k-means algorithm, k-medoids chooses k-datapoint as centers of clusters.

The k-prototypes are used as shape representative for each fruit category. Hence, the dimension of feature vector will be $k\,x\,n$ dimension, with k is number of prototypes used in the k-medoids clustering and n is the number of fruit categories.

Figure 3: Fruit Images In 32 Subcategories

4. EXPERIMENTAL EVALUATION

In this experiment, we demonstrate the feasibility of our proposed bag-of-shapes descriptor for the multi-class fruit classification problem, in which the classification performance is described in Subsection 4.4 and 4.5. Beforehand, we describe the dataset used in the experiment in Subsection 4.1, the construction of chain code in Subsection 4.2, and the shape association construction for each fruit subcategory in Subsection 4.3.

Journal of Theoretical and Applied Information Technology
15th March 2017. Vol.95. No 5

ISSN: 1992-8645 www.jatit.org E-ISSN: 1817-3195

4.1 Data

The fruit object of RGBD Object Dataset [22] is used in this experiment. The fruit images in the dataset is color images with a single fruit object on each image, captured in multi-view point. There are 7 fruit categories, namely apple, banana, lemon, lime, orange, peach, and pear. Each category consists of some fruit subcategories, giving total 32 fruit subcategories namely `Apple_1`, `Apple_2`, `Apple_3`, `Apple_4`, `Apple_5`, `Banana_1`, `Banana_2`, `Banana_3`, `Banana_4`, `Lemon_1`, `Lemon_2`, `Lemon_3`, `Lemon_4`, `Lemon_5`, `Lemon_6`, `Lime_1`, `Lime_2`, `Lime_3`, `Lime_4`, `Orange_1`, `Orange_2`, `Orange_3`, `Orange_4`, `Peach_1`, `Peach_2`, `Peach_3`, `Pear_1`, `Pear_2`, `Pear_3`, `Pear_4`, `Pear_5`, and `Pear_6`. Each fruit subcategories consists of 400-700 images approximately, giving total images of 21284 images. Figure 3 shows the sample of fruit subcategories.

4.2 Chain Code Construction

We conduct edge detection process to extract the contour of the object. In the edge detection process, we use Gaussian filter in Canny edge detection with the blur_radius = 5 and σ = -1. The threshold used in determining the edge is 0.4 for `threshold_high` and 0.04 for `threshold_low`.

Figure 4: Chain code string of some images of banana_1

Figure 5: Chain code string of some images of apple_1

Further, we conduct thinning process [24] to the detected edge in order to get one-pixel thickness. This is needed in the chain code construction, in which we trace the one-pixel thickness contour using contour tracing method [25] and further represent the chain code in the form of 8-connectivity neighborhood Freeman Chain Code. Figure 4 and Figure 5 show some results of chain code string of some images of banana_1 and apple_1, respectively.

4.3 Shape Association for Each Subcategory

In the fruit dataset of RGBD Object dataset [22], the fruit is located in roundtable and captured in 3 (three) viewpoints, namely 30°, 45°, and 60° from the horizon. This condition necessitates the use of multiple prototypes for each fruit instance to capture all the variations. For that purpose, in this work we use the method of K-medoids clustering [11] to select a set of representative prototypes from each fruit subcategory.

Beforehand, we apply the Needleman-Wunsch algorithm [26], [30] in the pairwise similarity calculation on each fruit subcategory, in order to get the shape association. Further, the shape association in the form of pairwise similarity matrix is used as the input for selecting k-prototypes in k-medoids clustering. In the experiment we used k-medoids implementation of ELKI [31].

Figure 6 and Figure 7 depicts five and ten prototypes, respectively, of some samples of fruit subcategory as the result of k-medoids clustering. It can be seen that our proposed method can get many variation in view of fruit subcategories. Further, the k-prototypes were use as features for each instance in the feature vector construction.

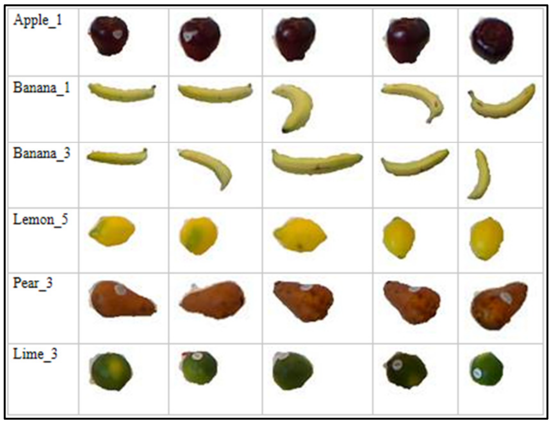

Figure 6: Sample of 5 prototypes of some fruit subcategory as the result of shape association step

4.4 Fruit Classification Result

We use nearest neighbor classifier, with 10-fold cross validation for the fruit classification. For this purpose, the feature vector is constructed from the result of shape association step (Subsection 4.3). Each prototype is used as attribute in the feature vector. For example, if we use 5 prototypes for each fruit subcategory, hence the feature vector will have 5 x 32 = 160 dimension, as we used 32 fruit subcategories in the experiment.

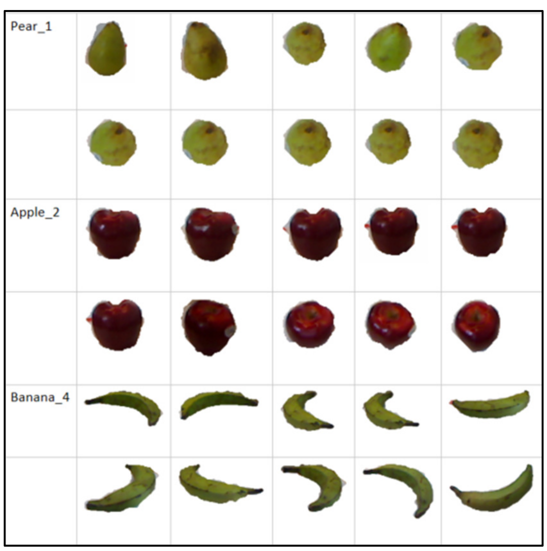

Figure 7: Samples of 10 prototypes of some fruit subcategories as the result of shape association step

The performance of classification was measured in terms of accuracy, TPR (True Positive Rate), and FPR (False Positive Rate), as described in (4), (5), and (6). We use TPR and FPR along with accuracy in order to emphasize that our fruit classification system did not get into accuracy paradox problem.

$$accuracy = \frac{TP + TN}{TP + TN + FP + FN} \quad (4)$$

$$TPR = \frac{TP}{TP + FN} \quad (5)$$

$$FPR = \frac{FP}{FP + TN} \quad (6)$$

with TP (True Positive) is the number of images correctly classified as belonging to the positive class (correctly classified), TN (True Negative) is the number of images correctly classified as belonging to the negative class (correctly rejected), FP (False Positive) is the number of images incorrectly classified as belonging to the class (incorrectly classified), and FN (False Negative) is the number of images which were not classified as belonging to the positive class but should have been (incorrectly rejected).

Table 1: The accuracy (acc) of proposed descriptor in fruit classification using different number of prototypes (k). Accuracy value is in percentage (%)

K	5	10	15	20	25	30
acc	75.53	78.16	81.31	82.28	82.65	82.96

As depicted in Table 1, the accuracy of fruit classification is increasing in accordance to the increasing number of prototypes. It suits our presumption that if the system could provide a suitable number of shape prototypes, the classification rate might be increased. This aspect is very importance in the classification system based on shape feature, as the same object will establish different shapes if the camera viewpoint used in capturing the object is different.

The accuracy of fruit classification in using 30 prototypes for each fruit subcategories achieves 82.96 %, along with TPR = 0.827 and FPR = 0.006. Based on those values and equation in (4), (5), and (6), it can be inferred that the value of True Negative (TN) and False Negative (FN) from our experiment is very small. Hence, the accuracy paradox can be avoided.

In Figure 9, and Figure 10, we depict the TPR and FPR of different number of prototypes (k), respectively. To identify the effect of choosing the number of prototypes in the classification, we use some different prototype values, namely 5, 10, 15, 20, 25, and 30. We apply Random Projection [32] to reduce feature dimensionality to improve classification speed, with the percentage of dimensions (attributes) the data should be reduced to is 75 %.

We show in Figure 9 that generally, `apple_2` get the lowest TPR, namely 0.666 for k = 30. This is due to the shape contour of prototypes of apple_2 have many similarities with prototype of other fruit objects, such as `apple_3`, `apple_5`, `orange_1`, `orange_2`. Hence, the FN (False Negative) is higher, resulting in the low value of TPR. Also, in constructing the prototypes, the k-medoids is applied to each fruit subcategory and is not paying attention to other fruit subcategory characteristic. On the other hand, the highest TPR is achieved by `pear_1`, namely 0.963 for k = 30. The prototypes of `pear_1` which is yielded from the shape association step (Subsection 4.3) is having high discriminative power, hence the FN is very low.

Meanwhile, the FPR value is ranging from 0.001 to 0.016, for all k values, as depicted in Figure 10. For k = 30, the highest FPR is achieved by `apple_3`, namely 0.009, while the lowest FPR is achieved by `banana_4`, namely 0.001. Generally, the prototypes of `apple_3` is rather similar to the prototypes of other fruit object due to the similarity in the shape contour. Whereas the prototypes of `banana_4` is very discriminative, as they represent many variations in shape contour of `banana_4`.

4.5 Comparative Analysis

Furthermore, we compare the accuracy of our method in fruit classification with chain code histogram (CCH) [17], as can be seen in Table 2. We use CCH as comparison since CCH is commonly used as shape descriptor of chain code based shape representation. We construct 8-bin CCH in this experiment.

Table 2: Performance comparison of Chain Code Histogram [17] and our work

Method	Accuracy	TPR	FPR
Chain Code Histogram [17]	47.36	0.474	0.017
This work	82.96	0.83	0.005

Our proposed bag-of-shapes descriptor performance is better than CCH (1-NN, 10-fold cross validation), in term of accuracy, namely 82.96 %, while the CCH only achieved 47.355 %. To achieve 82.96 % accuracy, we use k (prototypes) = 30. The low accuracy of CCH is due to CCH only calculate the distribution of chain code alphabet along the shape contour. As the same fruit object might establish different shape contour - as the effect of different viewpoint in capturing object by the camera-, the same fruit object will generate different CCH. In the classification process, it might be classified as different fruit object.

We give the TPR and FPR comparison of CCH and bag-of-shapes descriptor in fruit classification for each fruit subcategory, as can be seen in Figure 11 and Figure 12, respectively. As depicted in Figure 11, the number of images correctly classified is increasing with the use of bag-of shapes descriptor. In Table 3, we give the number of correctly and incorrectly classified fruit images, in the fruit classification using CCH or bag-of-shapes descriptor. In general, the number of correctly classified fruit images is increasing about 50 % by using bag-of-shapes descriptor.

Meanwhile, besides there are images that can be identified either using the CCH and the bag-of-shapes, there are also a number of images that can only be identified just by using CCH or bag-of shapes only. Table 4 shows the details. It can be seen that the use of bag-of-shapes descriptor able to increase the number of images which are correctly classified, significantly. Some examples of images that can be well identified by the bag-of-shapes descriptor but was not identified by CCH can be seen in Figure 15.

Table 3: Number of images correctly and incorrectly classified using CCH or bag-of-shapes descriptor.

fruit	CCH		bag-of-shapes	
	#correct	#incorrect	#correct	#incorrect
apple_1	295	312	502	105
apple_2	199	423	399	223
apple_3	169	438	401	206
apple_4	207	426	447	186
apple_5	228	401	527	102
banana_1	534	192	673	53
banana_2	546	168	583	131
banana_3	557	142	549	150
banana_4	529	158	653	34
pear_1	540	134	643	31
pear_2	361	308	553	116
pear_3	547	136	627	56
pear_4	482	182	595	69
pear_5	397	364	702	59

ISSN: 1992-8645 www.jatit.org E-ISSN: 1817-3195

fruit	CCH		bag-of-shapes	
	#correct	#incorrect	#correct	#incorrect
pear_6	297	438	571	164
peach_1	195	479	535	139
peach_2	448	256	622	82
peach_3	205	496	506	195
lime_1	228	402	520	110
lime_2	230	410	586	54
lime_3	188	414	469	133
lime_4	245	397	489	153
lemon_1	238	355	448	145
lemon_2	257	409	545	121
lemon_3	267	347	463	151
lemon_4	262	340	441	161
lemon_5	273	381	473	181
lemon_6	236	382	418	200
orange_1	245	465	590	120
orange_2	226	487	580	133
orange_3	174	533	516	191
orange_4	274	430	603	101

Table 4: Number of images correctly classified. The number of images correctly classified only by using CCH, only by using bag-of-shapes, and both approach can be seen in the column 'CCH', 'bag-of-shapes', and 'both', respectively

fruit subcategory	CCH	bag-of-shapes	both
apple_1	31	238	264
apple_2	42	242	157
apple_3	46	278	123
apple_4	48	288	159
apple_5	16	315	212
banana_1	22	161	512
banana_2	77	114	469
banana_3	96	88	461
banana_4	20	144	509
pear_1	5	108	535
pear_2	25	217	336
pear_3	18	98	529
pear_4	25	138	457
pear_7	13	318	384
pear_8	34	308	263
peach_1	17	357	178
peach_2	28	202	420
peach_3	27	328	178

fruit subcategory	CCH	bag-of-shapes	both
lime_1	31	323	197
lime_2	13	369	217
lime_3	25	306	163
lime_4	34	278	211
lemon_1	25	235	213
lemon_2	18	306	239
lemon_3	30	226	237
lemon_4	38	217	224
lemon_5	40	240	233
lemon_6	53	235	183
orange_1	31	376	214
orange_2	35	389	191
orange_3	30	372	144
orange_4	20	349	254

Furthermore, the use of bag-of-shapes descriptor also able to reduce misclassification on the banana category. It can be seen in the confusion matrix in Figure 14, all images of banana subcategory (banana_1, banana_2, banana_3, and banana_4) can be correctly classified. The misclassification on the banana still revolves around banana category also. In contrast to the use of CCH, there is still banana images misclassified into category other than banana, as shown in Figure 13.

Among others, the shape context [14] is very popular shape descriptor and commonly used for object recognition. In comparing with shape context, we also apply the k-medoids clustering to the pairwise similarity calculation of the shape context value. For our experiment, we use the shape context implementation of BoofCV [33]. Accuracy comparison of our proposed bag-of-shapes descriptor and shape context is presented in Table 5. It can be inferred from Table 5 that our proposed bag-of-shapes descriptor is better than shape context. This comparison is also depicted in Figure 8 to show clarity.

Table 5: Accuracy comparison of this work and shape context (SC) [14] using different number of prototype (k). All value is in percentage (%)

k	5	10	15	20	25	30
SC	47.84	59.55	66.00	70.54	72.63	74.41
This work	75.53	78.16	81.31	82.28	82.65	82.96

Meanwhile, we use Hu's moment in comparison as this method is used in the [34] as shape representation in fruit recognition and our work use the same dataset as in [34]. The accuracy in [34] is 72.04 %, slightly worse than accuracy in our proposed method, namely 82.96 %.

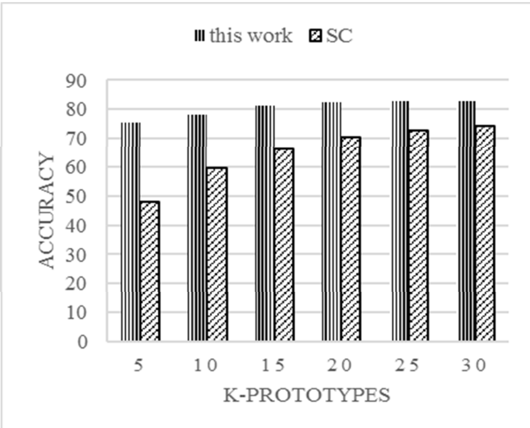

Figure 8: Accuracy (%) comparison of this work and shape context (SC) using different number of prototype

5. CONCLUSION AND FUTURE WORKS

We proposed a novel bag-of-shape descriptor using shape association, based on Freeman Chain Code. For the computation of shape association, we apply Needleman-Wunsch algorithm as commonly used in solving the sequence alignment problem. From the experiment on fruit dataset, our proposed method achieves better classification accuracy compared to conventional chain code based shape descriptor technique, namely Chain Code Histogram. Besides that, our proposed shape descriptor also surpassed the accuracy of shape descriptor already applied in multi-view fruit object recognition. Furthermore, we also show that selecting some shape prototypes for each fruit subcategory is an important process in the fruit recognition problem. As we may know that each shape will have a particular shape representation especially in chain code representation, hence it become necessary to have some representative shape representation of a particular fruit class. In our experiment, we successfully show that the application of k-medoids clustering on the likelihood association on chain code representation of fruit shape, can capture the diversity of shape variations of single fruit object.

Along with its success, in the resulting set of prototype we still find some prototypes which did not reflect the diversity of view of fruit object, such as in apple, lemon, and orange category, which produce low True Positive Rate. This condition is due to the chain code representation sometimes contains small noise, since the construction of chain code sometimes suffer from staircase-effect. We plan to improve this limitation, by applying the discrete contour evolution (DCE) technique to the shape contour in the chain code construction step in the future works. We also plan to use some threshold to refine the prototypes as the result of k-medoids clustering, by reducing the centroid (of k-medoids) which only have few members, in order to get the more appropriate prototypes of each fruit subcategory.

ACKNOWLEDGEMENT

We would like to thank Ministry of Research Technology and Higher Education of the Republic of Indonesia (Kementerian Riset Teknologi dan Pendidikan Tinggi Republik Indonesia) for the financial support in conducting this research.

REFERENCES

[1] D. Zhang and G. Lu, "Review of shape representation and description techniques," *Pattern Recognit.*, vol. 37, no. 1, pp. 1–19, 2004.

[2] F. Berrada, D. Aboutajdine, S. E. Ouatik, and a. Lachkar, "Review of 2D shape descriptors based on the curvature scale space approach," in *International Conference on Multimedia Computing and Systems -Proceedings*, 2011, no. 1, pp. 1–6.

[3] Y. Mingqiang, K. K. Idiyo, and R. Joseph, "A Survey of Shape Feature Extraction Techniques," *Pattern Recognition, Peng-Yeng Yin 43-90*, pp. 43–90, 2008.

[4] I. K. Kazmi, L. You, and J. J. Zhang, "A Survey of 2D and 3D Shape Descriptors," *2013 10th Int. Conf. Comput. Graph. Imaging Vis.*, pp. 1–10, Aug. 2013.

[5] A. N. Azmi and D. Nasien, "Feature vector of binary image using Freeman Chain Code (FCC) representation based on structural classifier," *Int. J. Adv. Soft Comput. its Appl.*, vol. 6, no. 2, pp. 1–19, 2014.

[6] J. Park, K. M. M. Chisty, J. Lee, Y. An, and Y. Choi, "Image retrieval technique using rearranged freeman chain code," in *Proceedings - 1st International Conference on Informatics and Computational Intelligence, ICI 2011*, 2011, pp. 283–286.

ISSN: 1992-8645 www.jatit.org E-ISSN: 1817-3195

[7] N. A. Jusoh and J. Mohamad Zain, "Malaysian Car Plates Recognition Using Freeman Chain Codes and Characters' Features," in *Software Engineering and Computer Systems: Second International Conference, ICSECS 2011, Kuantan, Pahang, Malaysia, June 27-29, 2011, Proceedings, Part I*, J. Mohamad Zain, W. M. bt Wan Mohd, and E. El-Qawasmeh, Eds. Berlin, Heidelberg: Springer Berlin Heidelberg, 2011, pp. 581–591.

[8] E. Rosch, C. B. Mervis, W. D. Gray, D. M. Johnson, and P. Boyes-Braem, "Basic objects in natural categories," *Cogn. Psychol.*, vol. 8, no. 3, pp. 382–439, 1976.

[9] M. Bar, "The proactive brain: using analogies and associations to generate predictions," *Trends Cogn. Sci.*, vol. 11, no. 7, pp. 280–289, 2007.

[10] H. Freeman, "On the Encoding of Arbitrary Geometric Configurations," *IEEE Trans. Electron. Comput.*, vol. EC-10, no. 2, pp. 260–268, Jun. 1961.

[11] L. Kaufman and P. J. Rousseeuw, "Clustering by Means of Medoids," in *Statistical Data Analysis Based on the L1-Norm and Related Methods*, 1987.

[12] T. Malisiewicz and A. A. Efros, "Recognition by association via learning per-exemplar distances," *26th IEEE Conf. Comput. Vis. Pattern Recognition, CVPR*, 2008.

[13] J. Hays and A. A. Efros, "Scene Completion Using Millions of Photographs," vol. 1, no. 212, pp. 1–7, 2007.

[14] S. Belongie, J. Malik, and J. Puzicha, "Shape matching and object recognition using shape contexts," *Pattern Anal. Mach. Intell. IEEE Trans.*, vol. 24, no. 4, pp. 509–522, Apr. 2002.

[15] H. Zhang and J. Malik, "Learning a Discriminative Classifier Using Shape Context Distances," in *IEEE Computer Society Conference on Computer Vision and Pattern Recognition*, 2003, p. I-242-I-247.

[16] Y. Yang and J. O. Pedersen, "A comparative study on feature selection in text categorization," *Mach. Learn. Work. Then Conf.*, pp. 412–420, 1997.

[17] J. Iivarinen and A. Visa, "Shape recognition of irregular objects," *Intell. Robot. Comput. Vis. XV ALGORITHMS, Tech. Act. VISION, Mater. Handl. PROC. SPIE 2904*, vol. 2904, pp. 25--32, 1996.

[18] J. Sun and H. Xu, "Contour-Shape recognition and retrieval based on chain code," in *CIS 2009 - 2009 International Conference on Computational Intelligence and Security*, 2009, vol. 1, pp. 349–352.

[19] J. Sun and X. Wu, "Chain Code Distribution-Based Image Retrieval," in *Proceedings of the 2006 International Conference on Intelligent Information Hiding and Multimedia*, 2006, pp. 139–142.

[20] J. Sun and X. Wu, "Shape Retrieval Based on the Relativity of Chain Codes," in *Multimedia Content Analysis and Mining: International Workshop, MCAM 2007, Weihai, China, June 30-July 1, 2007. Proceedings*, N. Sebe, Y. Liu, Y. Zhuang, and T. S. Huang, Eds. Berlin, Heidelberg: Springer Berlin Heidelberg, 2007, pp. 76–84.

[21] S. Li, A. Lum, G. Brahm, I. Ben Nachum, M. Sharma, O. Shmuilovich, and J. Warrington, "A Bag-of-shapes descriptor for medical imaging," in *2016 IEEE International Conference on Image Processing (ICIP)*, 2016, pp. 2316–2320.

[22] K. Lai, L. Bo, X. Ren, and D. Fox, "A large-scale hierarchical multi-view RGB-D object dataset," in *ICRA*, 2011, pp. 1817–1824.

[23] J. Canny, "A Computational Approach to Edge Detection," *IEEE Trans. Pattern Anal. Mach. Intell.*, vol. PAMI-8, no. 6, pp. 679–698, 1986.

[24] R. M. Haralick, T. Zhang, and C. Suen, "A fast parallel algorithm for thinning digital patterns," *Commun. ACM*, vol. 27, no. 3, pp. 236–239, 1984.

[25] F. Chang, C.-J. Chen, and C.-J. Lu, "A linear-time component-labeling algorithm using contour tracing technique," *Comput. Vis. Image Underst.*, vol. 93, no. 2, pp. 206–220, 2004.

[26] G. Navarro, "A guided tour to approximate string matching," *ACM Comput. Surv.*, vol. 33, no. 1, pp. 31–88, 2001.

[27] E. Rachmawati, M. L. Khodra, and I. Supriana, "Shape based Recognition Using Freeman Chain Code and Modified Needleman-Wunsch," in *The 8th 2016 International Conference on Information Technology and Electrical Engineering (ICITEE)*, 2016, pp. 461–466.

[28] M. Dayhoff and R. Schwartz, "A Model of Evolutionary Change in Proteins," in *In*

Atlas of protein sequence and structure, 1978, pp. 345–352.

[29] S. Henikoff and J. G. Henikoff, "Amino acid substitution matrices from protein blocks.," *Proc. Natl. Acad. Sci. U. S. A.*, vol. 89, no. 22, pp. 10915–10919, 1992.

[30] Sam Chapman, "SimMetrics: A Java library of similarity and distance metrics." 2009.

[31] E. Schubert, A. Koos, T. Emrich, A. Züfle, K. A. Schmid, and A. Zimek, "A Framework for Clustering Uncertain Data," *PVLDB*, vol. 8, no. 12, pp. 1976–1979, 2015.

[32] D. Fradkin and D. Madigan, "Experiments with random projections for machine learning," in *Proceedings of the ninth ACM SIGKDD international conference on Knowledge discovery and data mining*, 2003, pp. 517–522.

[33] P. Abeles, "BoofCV." 2012.

[34] L. Jiang, A. Koch, S. A. Scherer, and A. Zell, "Multi-class fruit classification using RGB-D data for indoor robots," in *2013 IEEE International Conference on Robotics and Biomimetics (ROBIO)*, 2013, pp. 587–592.

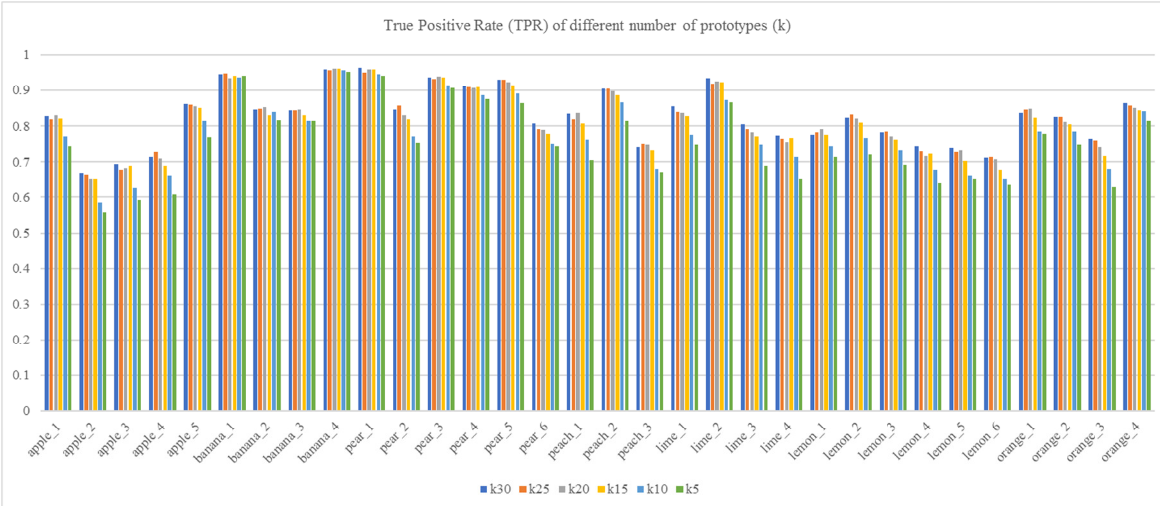

Figure 9: TPR of fruit classification using different number of prototypes (k)

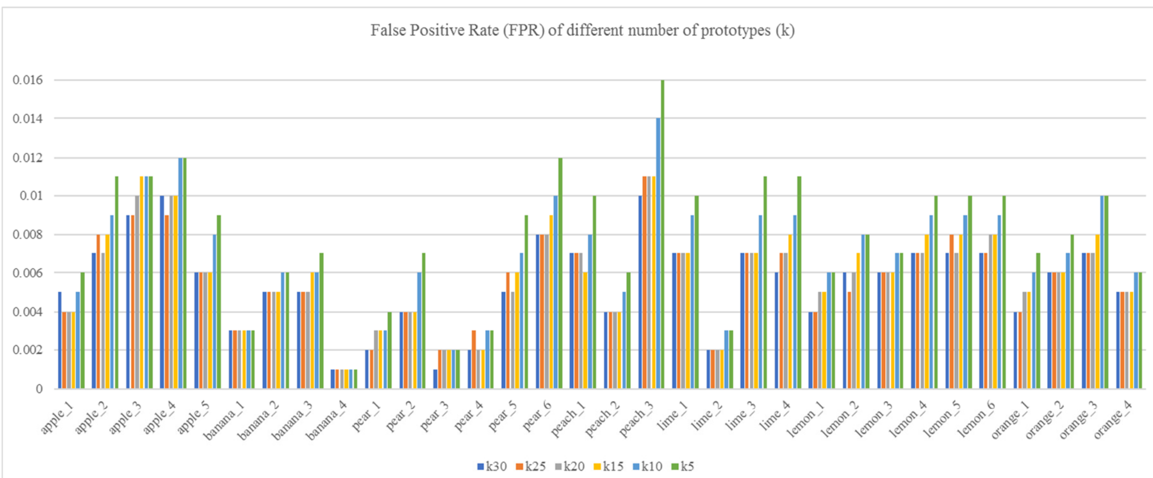

Figure 10: FPR of fruit classification using different number of prototypes (k)

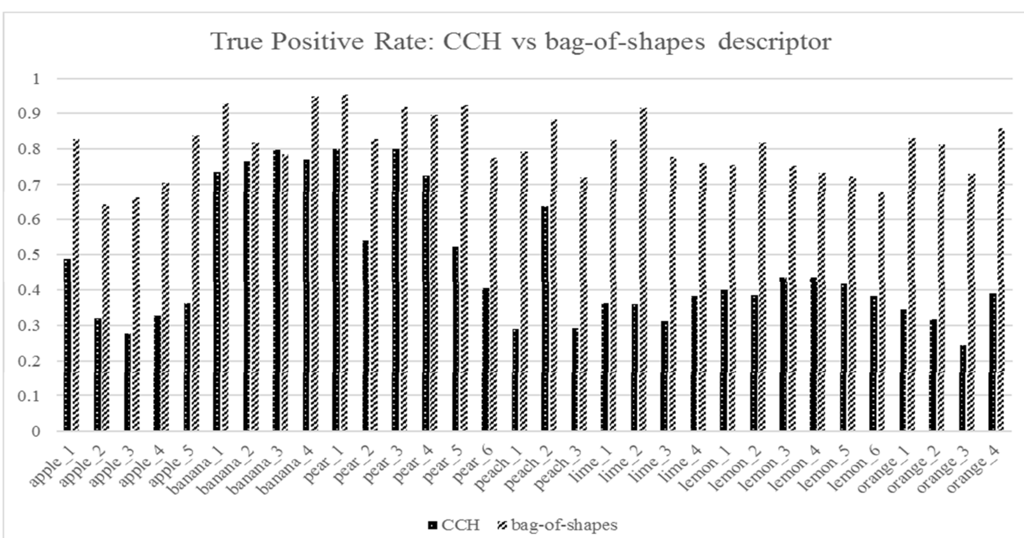

Figure 11: TPR comparison of fruit classification using Chain Code Histogram vs bag-of-shapes descriptor

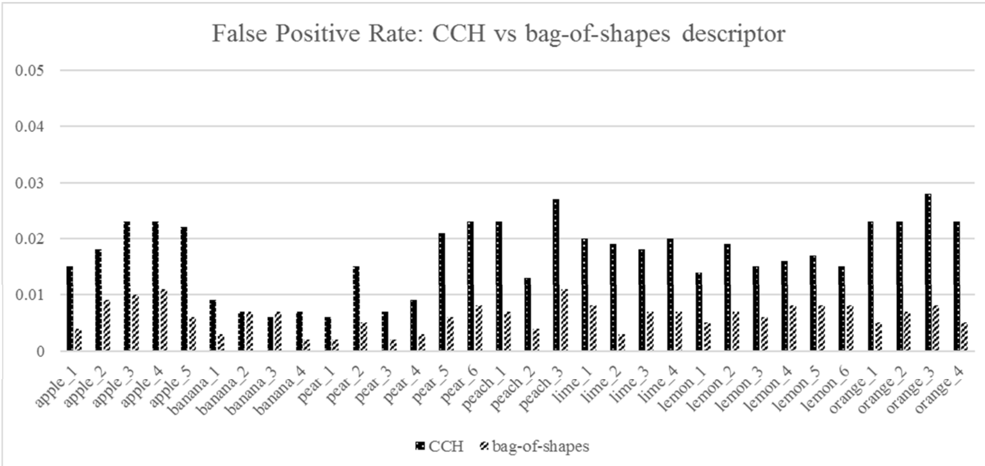

Figure 12: FPR comparison of fruit classification using Chain Code Histogram vs bag-of-shapes descriptor

a	b	c	d	e	f	g	h	i	j	k	l	m	n	o	p	q	r	s	t	u	v	w	x	y	z	aa	ab	ac	ad	ae	af	<-- classified as
295	70	37	57	10	1	1	1	1	4	4	2	1	6	7	6	1	13	5	5	0	3	1	4	7	4	3	2	10	6	11	29	a = apple_1
77	199	67	76	17	2	1	0	3	2	5	0	3	3	15	13	13	16	7	8	7	2	1	7	6	14	8	3	6	8	7	26	b = apple_2
36	57	169	62	26	2	0	0	0	1	7	0	2	7	30	23	8	20	11	11	5	12	1	2	6	7	8	1	16	20	28	29	c = apple_3
52	55	63	207	19	0	0	0	1	4	1	0	2	2	12	15	11	31	5	8	6	5	4	2	10	14	9	4	8	15	24	44	d = apple_4
7	8	24	16	228	4	0	0	0	1	7	1	11	30	48	28	7	31	16	11	20	5	3	5	7	7	1	2	32	21	34	14	e = apple_5
1	1	2	0	6	534	21	11	36	1	7	1	0	4	3	3	6	0	2	5	2	10	16	11	4	2	11	17	6	0	1	2	f = banana_1
2	2	1	1	1	21	546	85	11	6	5	4	3	0	0	0	0	0	1	3	1	1	2	1	4	3	2	5	0	0	3	0	g = banana_2
1	1	0	0	0	12	77	557	10	4	0	12	0	0	0	0	1	0	1	1	2	2	2	2	2	3	3	5	1	0	0	0	h = banana_3
2	2	0	1	2	41	9	8	529	1	1	6	0	1	2	1	5	0	1	0	0	5	23	10	8	6	8	7	2	1	0	5	i = banana_4
0	6	3	5	1	3	7	0	0	540	31	4	0	7	5	3	1	8	3	3	0	3	0	1	1	5	0	3	1	9	10	11	j = pear_1
2	8	4	4	12	8	0	0	2	32	361	0	6	19	3	21	1	12	13	21	10	10	7	9	11	22	11	6	15	15	17	7	k = pear_2
2	0	0	0	1	4	2	7	7	8	1	547	34	4	8	3	5	0	9	2	5	1	3	3	9	5	3	3	5	1	1	0	l = pear_3
2	1	1	1	7	1	1	0	1	1	9	43	482	5	7	5	6	5	7	4	7	11	2	6	8	9	9	3	4	8	6	2	m = pear_4
5	3	8	6	34	2	0	0	0	6	14	4	4	397	44	30	10	20	11	10	28	14	2	4	7	4	3	3	39	10	25	14	n = pear_5
6	9	19	6	54	2	0	0	0	3	5	7	9	43	297	28	5	54	8	8	16	9	3	7	0	3	1	5	27	21	51	29	o = pear_6
4	7	22	21	30	2	0	0	0	8	16	3	6	35	30	195	8	38	16	18	14	9	7	10	9	8	7	10	26	53	36	26	p = peach_1
4	14	10	10	3	2	0	0	2	0	2	7	10	8	10	7	448	5	28	13	11	11	7	29	4	9	5	6	32	4	3	0	q = peach_2
13	14	23	28	36	1	0	0	0	3	6	1	3	22	53	35	3	205	9	14	4	5	5	9	8	3	2	2	17	56	73	48	r = peach_3
1	9	16	5	22	2	0	1	1	4	14	7	8	16	17	13	23	12	228	19	43	42	13	25	15	11	6	2	30	6	13	6	s = lime_1
5	8	13	9	9	2	2	1	1	3	23	3	7	9	11	19	11	25	32	230	26	36	13	20	12	12	18	6	39	13	12	10	t = lime_2
5	7	5	9	24	1	1	1	0	1	13	7	12	40	20	19	15	7	49	21	188	34	7	26	8	11	7	6	33	12	9	4	u = lime_3
10	6	17	5	3	6	1	0	3	0	6	0	8	14	7	7	16	8	40	42	44	245	10	29	19	18	14	10	26	10	9	9	v = lime_4
4	6	5	2	4	23	1	2	22	1	10	4	3	3	2	9	6	6	19	13	7	17	238	25	20	27	43	51	7	1	6	6	w = lemon_1
3	6	4	6	3	4	2	1	11	2	13	2	5	11	9	20	21	7	33	25	25	34	23	257	14	19	20	25	21	16	14	10	x = lemon_2
18	11	12	9	5	5	4	0	9	1	8	5	4	11	3	7	8	3	12	16	14	23	26	23	267	21	38	27	8	3	4	9	y = lemon_3
4	7	2	17	9	5	1	0	9	2	26	4	8	8	5	7	11	6	15	15	9	17	22	28	19	262	23	33	8	6	6	8	z = lemon_4
4	11	13	7	4	10	0	4	11	0	9	0	10	5	4	10	8	7	14	14	13	17	33	22	41	26	273	58	7	6	7	6	aa = lemon_5
4	9	8	8	2	15	1	2	8	6	11	3	4	5	7	8	8	2	5	7	6	18	50	28	29	41	65	236	4	6	5	7	ab = lemon_6
7	7	18	7	37	4	1	1	1	1	13	7	5	55	24	23	37	18	26	33	32	24	5	14	6	6	4	5	245	14	18	12	ac = orange_1
8	12	26	19	22	1	1	0	0	7	15	1	3	15	30	50	3	68	5	17	15	6	1	8	6	4	6	2	12	226	77	47	ad = orange_2
10	10	27	27	35	1	1	0	1	7	11	0	4	23	45	27	3	89	8	13	7	10	4	5	5	6	5	5	19	70	174	55	ae = orange_3
13	15	25	47	17	1	0	0	2	8	9	0	2	16	18	24	0	53	5	8	2	8	4	11	2	3	4	3	11	56	63	274	af = orange_4

Figure 13: Confusion matrix of classification result using CCH

a	b	c	d	e	f	g	h	i	j	k	l	m	n	o	p	q	r	s	t	u	v	w	x	y	z	aa	ab	ac	ad	ae	af	<-- classified as
502	23	26	9	6	0	0	0	0	0	4	0	0	0	0	0	0	1	0	0	0	0	0	0	0	0	0	0	1	14	20	1	a = apple_1
26	399	61	85	11	0	0	0	0	0	9	0	3	7	1	0	0	9	0	0	0	0	0	0	0	0	0	0	6	4	1	0	b = apple_2
19	50	401	74	8	0	0	0	0	0	0	0	0	2	10	0	0	19	0	0	0	0	0	0	0	0	0	0	6	8	10	0	c = apple_3
15	61	61	447	17	0	0	0	0	0	2	0	3	5	1	0	0	8	0	0	0	0	0	0	0	0	0	0	3	4	6	0	d = apple_4
3	9	9	19	527	0	0	0	0	0	4	0	4	18	1	0	1	1	0	0	0	0	0	1	0	0	0	0	15	5	12	0	e = apple_5
0	0	0	0	0	673	15	19	19	0	0	0	0	0	0	0	0	0	0	0	0	0	0	0	0	0	0	0	0	0	0	0	f = banana_1
0	0	0	0	0	14	583	112	5	0	0	0	0	0	0	0	0	0	0	0	0	0	0	0	0	0	0	0	0	0	0	0	g = banana_2
0	0	0	0	0	27	115	549	8	0	0	0	0	0	0	0	0	0	0	0	0	0	0	0	0	0	0	0	0	0	0	0	h = banana_3
0	0	0	0	0	22	6	6	653	0	0	0	0	0	0	0	0	0	0	0	0	0	0	0	0	0	0	0	0	0	0	0	i = banana_4
0	0	0	0	0	0	0	0	0	643	8	0	1	2	0	3	2	0	2	0	0	4	0	2	1	1	5	0	0	0	0	0	j = pear_1
3	6	3	4	4	0	0	0	0	21	553	0	0	6	0	17	2	0	3	0	1	5	1	12	3	6	7	1	6	2	3	0	k = pear_2
0	0	0	0	0	0	0	0	0	0	0	627	28	3	0	4	6	0	0	0	0	0	2	3	1	3	2	2	2	0	0	0	l = pear_3
0	1	0	1	6	0	0	0	0	0	0	26	595	8	0	0	1	0	0	0	0	0	0	7	1	2	0	0	16	0	0	0	m = pear_4
0	3	0	0	9	0	0	0	0	0	7	0	2	702	0	3	3	0	0	0	0	0	0	7	1	3	0	4	17	0	0	0	n = pear_5
0	1	8	2	1	0	0	1	0	0	0	0	0	0	571	0	0	88	0	0	0	0	0	0	0	0	0	0	0	18	21	24	o = pear_6
0	0	0	0	0	0	0	0	0	7	7	0	2	9	0	535	4	0	20	15	14	15	4	8	10	10	9	5	0	0	0	0	p = peach_1
0	0	0	0	0	0	0	0	0	0	6	1	0	14	0	2	622	0	0	0	0	1	2	16	4	16	8	5	7	0	0	0	q = peach_2
3	9	17	9	1	0	0	0	0	0	0	0	0	0	84	0	0	506	0	0	0	0	0	0	0	0	0	0	0	14	17	41	r = peach_3
0	0	0	0	0	0	0	0	0	0	1	0	0	0	0	14	2	0	520	7	52	25	5	0	0	1	3	0	0	0	0	0	s = lime_1
0	0	0	0	0	0	0	0	0	0	0	0	0	0	0	18	0	0	9	586	16	11	0	0	0	0	0	0	0	0	0	0	t = lime_2
0	0	0	0	0	0	0	0	0	1	2	0	0	0	0	15	0	0	48	21	469	41	3	0	0	2	0	0	0	0	0	0	u = lime_3
0	0	0	0	0	0	0	0	0	3	3	1	0	0	0	13	1	0	41	8	51	489	15	1	4	4	6	2	0	0	0	0	v = lime_4
0	0	0	0	0	0	0	0	0	4	3	0	0	0	0	12	4	0	17	2	10	29	448	4	11	10	21	18	0	0	0	0	w = lemon_1
0	1	0	4	2	0	0	0	0	4	16	0	6	13	0	2	17	0	2	0	0	3	1	545	13	15	7	7	8	0	0	0	x = lemon_2
0	0	0	0	0	0	0	0	0	3	4	2	1	4	0	12	6	0	2	0	0	5	10	23	463	27	25	26	1	0	0	0	y = lemon_3
0	0	0	0	0	0	0	0	0	0	7	2	2	3	0	12	13	0	7	0	3	4	6	18	22	441	18	44	0	0	0	0	z = lemon_4
0	0	0	0	0	0	0	0	0	1	4	0	0	2	0	21	5	0	10	0	0	7	32	12	19	21	473	47	0	0	0	0	aa = lemon_5
0	0	0	0	0	0	0	0	0	3	3	2	1	6	0	4	14	0	0	0	0	2	16	13	24	51	57	418	4	0	0	0	ab = lemon_6
3	4	9	5	27	0	0	0	0	0	5	0	10	28	0	0	7	1	0	0	0	0	0	8	0	0	0	1	590	2	10	0	ac = orange_1
9	6	6	3	3	0	0	0	0	0	0	0	0	0	17	0	0	22	0	0	0	0	0	0	0	0	0	0	3	580	49	15	ad = orange_2
10	2	11	5	20	0	0	0	0	0	1	0	0	0	29	0	0	31	0	0	0	0	0	0	0	0	0	0	9	54	516	19	ae = orange_3
1	0	0	0	0	0	0	0	0	0	0	0	0	0	29	0	0	46	0	0	0	0	0	0	0	0	0	0	0	12	13	603	af = orange_4

Figure 14: Confusion matrix of classification result using bag-of-shapes descriptor

ISSN: 1992-8645 www.jatit.org E-ISSN: 1817-3195

Figure 15: Samples of fruit images which can be identified by using bag-of-shapes descriptor but misidentified by using chain code histogram